Polymer 50 (2009) 5787–5793

Contents lists available at ScienceDirect

Polymer

journal homepage: www.elsevier.com/locate/polymer

# A facile gemini surfactant-improved dispersion of carbon nanotubes in polystyrene

Guoxing Sun [a,b], Guangming Chen [a,*], Jun Liu [a,c], Jiping Yang [c], Jianyun Xie [c], Zhengping Liu [b,*], Ru Li [a], Xin Li [d]

[a] Beijing National Laboratory for Molecular Sciences (BNLMS), Laboratory of New Materials and State Key Laboratory of Polymer Physics and Chemistry, Institute of Chemistry, The Chinese Academy of Sciences, Beijing 100190, PR China
[b] Institute of Polymer Chemistry and Physics of College of Chemistry, BNU Key Lab of Environmentally Friendly and Functional Polymer Materials, Beijing Normal University, Beijing 100875, PR China
[c] Key Laboratory of Aerospace Materials and Performance (Ministry of Education), School of Materials Science and Engineering, Beihang University, Beijing 100191, PR China
[d] Beijing Key Laboratory of Clothing Materials R D and Assessment, Beijing Institute of Clothing Technology, Beijing 100029, PR China

ARTICLE INFO

*Article history:*
Received 14 June 2009
Received in revised form
11 August 2009
Accepted 3 October 2009
Available online 9 October 2009

*Keywords:*
Carbon nanotubes
Polystyrene (PS)
Gemini surfactant

ABSTRACT

Debundling and dispersion of carbon nanotubes (CNTs) are very important for preparation of polymer/CNT nanocomposites. In the present study, a self-prepared gemini surfactant, 6,6′-(butane-1,4-diylbis(oxy))bis(3-nonylbenzenesulfonic acid), is employed to achieve homogeneous and stable dispersion of multi-walled carbon nanotubes (MWNTs) in organic solvent and subsequent polystyrene (PS)/MWNT nanocomposite. Sedimentation, optical microscopy and transmission electron microscopy studies demonstrate that the gemini surfactant can greatly improve the dispersion and stabilization of MWNTs in toluene. Scanning electron microscopic images clearly confirm the homogenous dispersion of individual MWNTs in PS. In addition, desired enhanced electrical conductivity and thermal stability of the nanocomposite relative to those of the neat PS are obtained.



## 1. Introduction

Since their discovery in 1991 [1], carbon nanotubes (CNTs) have become a focus in chemistry, physics and material science due to their superior mechanical [2], electrical [3] and thermal [4] properties. Effective utilization of these exciting properties in polymer based composites mainly depends on their dispersion and interfacial interaction. Unfortunately, because of their high aspect ratios, large specific surface area, and substantial van der Waals attractions, CNTs tend to self-aggregate into bundles spontaneously [5]. To date, oxidation or fluorination [6–9], covalent functionalization by organic molecules or polymers [10–14], and noncovalent wrapping by surfactants [15–20] or polymers [21–25] are major techniques developed to improve the CNT dispersion or solubilization. Compared with the aggressive oxidation, fluorination and covalent functionalization methods using strong acids and multi-step complex reactions, noncovalent wrapping provides a simple and easily-controlled way with obvious advantages of significantly reduced tube breakage, defect formation, and continuous π network disruption [23,26–28]. Our interest focuses on surfactant-improved CNT dispersion. Herein, we report a new facile gemini surfactant-improved dispersion of multi-walled carbon nanotubes (MWNTs) in toluene and subsequent dispersion in polystyrene (PS). Aided by the gemini surfactant, MWNTs were debundled and homogeneously dispersed in toluene evidenced by sedimentation, optical microscopy and transmission electron microscopy (TEM). Then, the PS/MWNT nanocomposite was obtained via solution mixing procedure. Finally, its structure was confirmed by scanning electron microscopy (SEM), and the electrical, thermal and mechanical properties were studied.

Gemini surfactant is a new class of surfactants consisting of at least two hydrophobic chains and two hydrophilic moieties connected by a spacer group. Despite its unique structure, it has attractive properties such as low critical micelle concentration (CMC) and high surface or interfacial activity [29–33]. Unfortunately, there have been no reports of polymer/CNT nanocomposites based on gemini surfactant-modified CNTs in our literature survey. In this study, we use a self-prepared gemini surfactant, 6,6′-(butane-1,4-*diyl*bis(oxy))*bis* (3-nonylbenzenesulfonic acid) (9BA-4-9BA), whose preparation is described in our previous report [34]. Its desired molecular structure, as shown in Scheme 1, was specially designed to meet the following necessities for PS/CNT system and the

* Corresponding authors. Tel.: +86 10 62560722.
*E-mail addresses:* chengm@iccas.ac.cn (G. Chen), lzp@bnu.edu.cn (Z. Liu).

0032-3861/$ – see front matter © 2009 Elsevier Ltd. All rights reserved.
doi:10.1016/j.polymer.2009.10.007

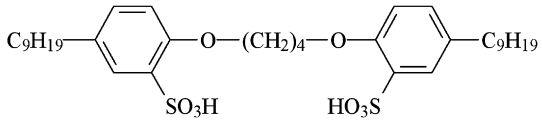


**Scheme 1.** The molecular structure of the gemini surfactant, 6.6′-(butane-1,4-diylbis(oxy))bis(3-nonylbenzenesulfonic acid) (9BA-4-9BA).

solution mixing process: 1) two phenyl rings are introduced since their π-π interaction with CNTs improves the ability of CNT dispersion and stabilization, and the interaction with the phenyl ring of the side groups of PS [16,28]; 2) butyl group in the spacer helps to increase the solubility in toluene (also a good solvent of PS) and the hydrophobicity; 3) the long alkyl chains ($C_9H_{19}$) favour to increasing the hydrophobic interaction and miscibility with PS. Note that the alkyl chain length can be neither too short (the extent of increase of the hydrophobic interaction and the miscibility is not enough) nor too long (the thermal stability may be deteriorated). To our knowledge, this is the first report on dispersion of CNTs in organic solvent using gemini surfactant, and then preparation of polymer/CNT nanocomposites, although enhancement of MWNT dispersion in aqueous solution by cationic gemini surfactant, hexyl-α,β-bis(dodecyldimethylammonium bromide) [35] or trimethylene-1,3-bis(dodecyldimethyl ammonium bromide) [36], has been reported.

## 2. Experimental part

### 2.1. Materials

The MWNTs used here are commercial baytubes C 150 P from Bayer, Germany, produced in a high-yield catalytic process based on chemical vapor deposition (CVD). Table 1 illustrates the product specifications provided by Bayer. The TEM image (Fig. 1) of MWNTs (ultrasonication in acetone) shows that the MWNTs are of higher purity, although some catalyst particles are still observed. PS (trademark 666D) was provided by Yanshan Petrochemicals Company, China. Toluene was bought from Beijing Chemical Corporation. Nonylphenol (NP) and chlorosulfonic acid (Beijing Chemical Engineering Factory, China) were stored at low temperature prior to use. 1,4-dibromobutane was bought from Shanghai Chemical Reagent Company, China. All of the other reagents are of analytical reagent (A.R.) pure grade.

### 2.2. Preparation of gemini surfactant

The gemini surfactant, 9BA-4-9BA, was prepared according to our previous report [34]. In brief, 2.5-fold molar excess of dibromobutane was added into the mixture of NP with the phase transfer catalyst (tetra-*n*-butylammonium bromide) in 20 wt% sodium hydroxide (NaOH) at 70 °C under stirring. The system reacted at 95 °C for 4 h under mechanically stirring. The resultant mixture was extracted using ether for three times at room temperature and washed by 3% glacial acetic acid and distilled water. Then, the diethers (I) were obtained by evaporating the solvent; 2.1-fold molar excess of chlorosulfonic acid was added into the diether (I) solution in anhydrous dichloromethane ($CH_2Cl_2$) at 0 °C and drop-wisely for 1 h under stirring. After 5 h of reaction, the solution was purged by nitrogen for 1 h to blow out the resulting hydrochloric acid and the rest chlorosulfonic acid. Finally, petroleum ether was added into the reaction solution to afford the raw surfactant residue, which was dissolved in dichloromethane and precipitated by petroleum ether for three times and dried under vacuum for 48 h at 40 °C.

**Table 1**
The product specifications of the used MWNTs.

| Property | Value | Unit | Method |
|---|---|---|---|
| C-Purity | >95 | % | Elementary analysis |
| Free amorphous carbon | Not detectible | % | TEM |
| Number of walls | 3–15 | – | TEM |
| Outer mean diameter | 13–16 | nm | TEM |
| Outer diameter distribution | 5–20 | nm | TEM |
| Inner mean diameter | 4 | nm | TEM |
| Inner diameter distribution | 2–6 | nm | TEM |
| Length | 1–>10 | μm | SEM |
| Apparent density | 140–160 | kg/m$^3$ | EN ISO 60 |
| Loose agglomerate size | 0,3–1 | mm | PSD |

### 2.3. Dispersion of MWNTs in toluene

Typically, 1 mg MWNTs were dispersed in 10 mL toluene. The dispersion with or without the presence of 10 mg gemini surfactant, was first homogenized by a high-shear homogenizer for 2 min, ultrasonicated for 1 h, and then stood for 1 week for dispersion characterization.

### 2.4. Preparation of PS/MWNT nanocomposites or composites

Fig. 2 shows the schematic representation of the preparation process of the PS/MWNT nanocomposite aided by the gemini surfactant via solution mixing. Large bundles of bare MWNTs are prevalent due to the strong van der Waals interactions (Fig. 2A). The hydrophilic –$SO_3H$ groups help the gemini surfactant form micelles in toluene, which are adorbed on MWNT surface due to interaction of the phenyls of the gemini surfactant with π electrons of MWNTs. As a result, the MWNTs bundles could be exfoliated into individual nanotubes and dispersed in the organic solvent (Fig. 2B), wherein the ratio of MWNT:9BA-4-9BA:toluene is 1 mg:5 mg:10 mL. Then, the stable homogeneous dispersion of the MWNT/9BA-4-9BA/toluene was added into PS/toluene solution at boiling state, and refluxed for 30 min. In this step, PS was dissolved in the MWNT/toluene system (Fig. 2C). After that, the mixture was slowly added into ethanol to precipitate. Finally, the products were filtrated, washed, and dried under vacuum overnight. In the PS/MWNT nanocomposites, individual MWNTs were dispersed homogeneously in the PS matrix (Fig. 2D). For comparison, PS/MWNT composites were also prepared by a similar process in the absence of the 9BA-4-9BA surfactant.

### 2.5. Dispersion characterization

The effect of the 9BA-4-9BA on dispersion of MWNTs in toluene was studied by sedimentation experiment, optical microscopy and TEM techniques. Photographs of the sedimentation tests were

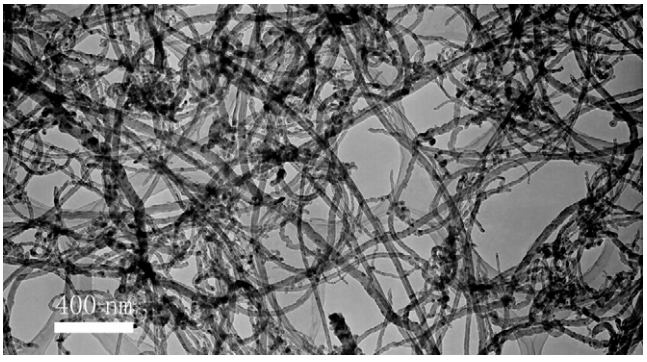


**Fig. 1.** TEM image of the bare MWNTs.

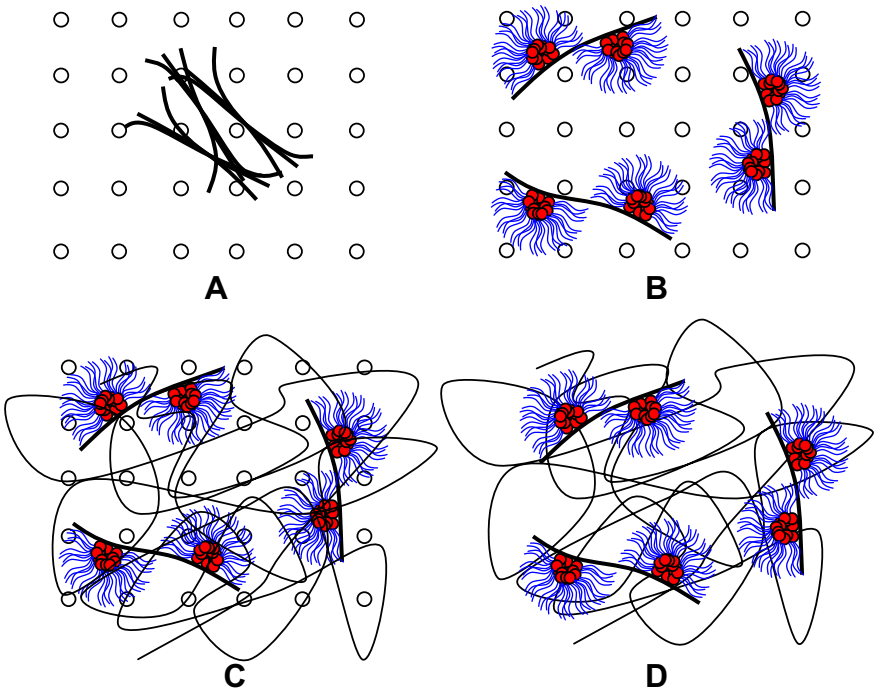


**Fig. 2.** Schematic representation of the preparation process of the PS/MWNT nanocomposites. The black thick bars, open circles, red circles with blue tails and curved lines represent MWNTs, solvent molecules, gemini surfactant and polymer chains, respectively.

taken by digital camera. The MWNT dispersions were deposited on glass slides to obtain film samples for optical microscopic observation by a LEICA DMIP microscope. TEM was performed on a JEM-2011 instrument measured at 100.0 kV, in which the sample was prepared by depositing the upper MWNT supernatants on copper grids and subsequent evaporating the solvent.

SEM was carried out to observe the debundling and dispersion state of MWNTs in PS on a HITACHI S-4300 instrument measured at 15.0 kV, with the samples snapped in a liquid nitrogen bath.

### 2.6. Soxhlet extraction and subsequent FTIR characterization

To study whether the gemini surfactant still remained in the as-prepared PS/MWNT nanocomposite and the amount of the 9BA-4-9BA, Soxhlet extraction experiment was conducted using ethanol as solvent. 0.541 g PS/MWNT nanocomposite was used for the extraction. The extraction time is 48 h. The extracted solution was further concentrated for FTIR spectra characterization, recorded on a Perkin–Elmer System 2000 FTIR spectrophotometer ranged 4000–400 $cm^{-1}$ at a nominal resolution of 4 $cm^{-1}$. In addition, after the Soxhlet extraction, the mass of the remained nanocomposite was weighed to calculate the amount of the 9BA-4-9BA left in the PS/MWNT nanocomposite.

### 2.7. Property measurements

Four-probe measurement using a Keithley 6221/2182A Delta Mode System was conducted to obtain the conductivity of the PS/MWNT nanocomposite or composite film with a thickness of around 10 μm.

Thermogravimetric analysis (TGA) was performed under nitrogen atmosphere using a Perkin–Elmer thermogravimetric analyzer, Pyris System, scanning from 30 to 800 °C at a heating rate of 20 or 10 °C/min.

Mechanical tensile tests were carried out on an Instron 3365P7573 material test system, measuring at 23% humidity and 25 °C. The film samples are about $50.0 \times 5.0 \times 0.20\ mm^3$. The tensile speed is 1.0 mm/min.

## 3. Results and discussion

### 3.1. Gemini surfactant dispersion in toluene

The effect of the gemini surfactant on dispersion of MWNTs was first studied by sedimentation tests. In sharp contrast to the bare MWNTs (Fig. 3A), which have obvious precipitations at the bottom, the gemini surfactant, 9BA-4-9BA, thanks to its benzene rings, favours the dispersion of MWNTs. A uniform black dispersion is

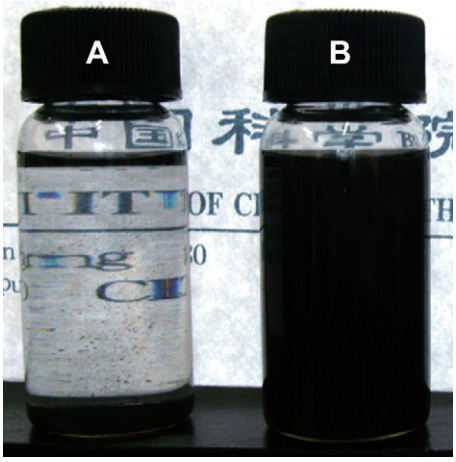


**Fig. 3.** Photograph of Vials of MWNT dispersions in toluene after 1 week containing: A) 1 mg MWNTs + 10 mL toluene; B) 1 mg MWNTs + 10 mg 9BA-4-9BA + 10 mL toluene.

clearly visible, neither precipitation nor aggregation can be observed (Fig. 3B). The 9BA-4-9BA might be adsorbed on and had a strong interaction with the surface of MWNTs, and the homogeneous MWNT dispersions were stabilized by micelles that covered the MWNT surface.

Then, the enhanced MWNT dispersion by the 9BA-4-9BA was further confirmed by optical microscopy and TEM techniques. In Fig. 4A, a high degree of nanotube aggregation can be clearly observed, and large agglomerates dominate. Their diameter ranges from several dozens to about 200 μm. To our delight, the 9BA-4-9BA yields no obvious large agglomerates of MWNTs as shown in Fig. 4B. Fig. 5 shows the TEM images, in which the black lines stand for MWNTs. Bundles are obvious in Fig. 5A, showing that the pristine MWNTs cannot be debundled and homogenously dispersed in toluene. However, after adding the gemini surfactant, MWNTs are dramatically debundled and well dispersed as individual CNTs, along with some catalyst particles (Fig. 5B). These results provide further evidences that 9BA-4-9BA can greatly improve the debundling and dispersion of MWNTs in toluene, which is consistent with the above sedimentation experiment very well.

### 3.2. PS/MWNT nanocomposite dispersion characterization

Based on the effective dispersion of MWNTs in toluene aided by the 9BA-4-9BA, polymer/MWNT nanocomposites are desired by a simple solution blending procedure. Here we choose PS, a widely used commercial thermoplastic resin which can be dissolved in toluene very well. The dispersion state of the MWNTs in the nanocomposite was examined by SEM images (Fig. 6). The white bars and points (pointed by arrows of "a" in Fig. 6D) represent MWNTs. In Fig. 6A, individual MWNTs cannot be observed in most areas and large bundles are discernible. The bundle pointed by an arrow in Fig. 6A is clearer in Fig. 6C with high magnification, which is made up of more than ten MWNTs. Interestingly, in Fig. 6B and D, numerous individual MWNTs are clearly prevalent. No agglomerates can be recognized. Besides, there are a few holes (pointed by arrows of "b" in Fig. 6D), resulting from the pulling out by the MWNTs during the SEM sample preparation. These SEM images strongly support that the 9BA-4-9BA can be used to effectively debundle and disperse the MWNTs in toluene, and further prepare PS/MWNT nanocomposite. Relative to the oxidative and covalent functionalization of the MWNTs, this study provides a new facile and effective preparation route.

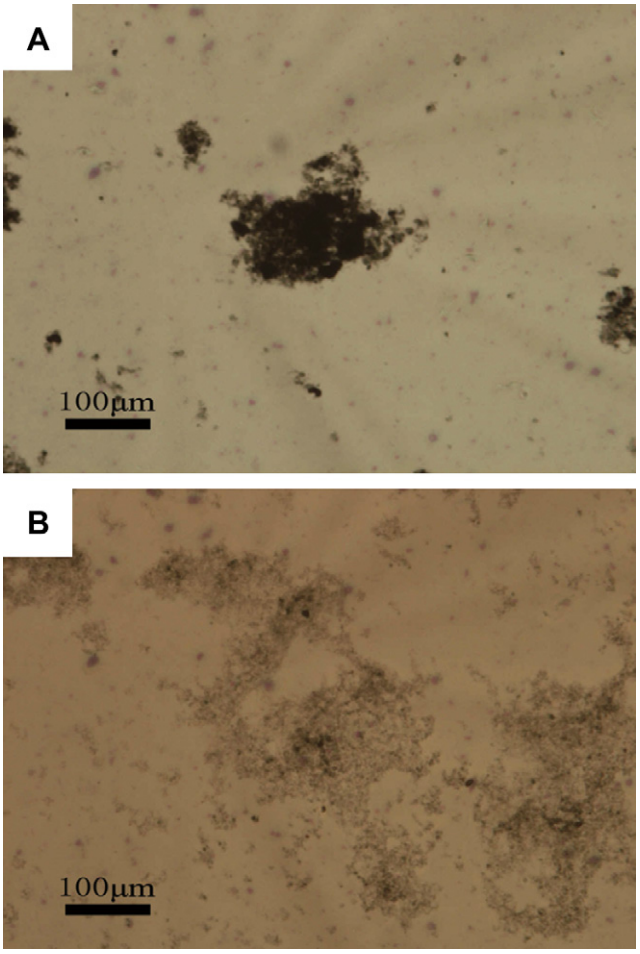


**Fig. 4.** Optical microscopy micrographs of dried MWNT dispersions after high-shear homogenizing, ultrasonication in toluene: A) without any dispersant; B) with 9BA-4-9BA as dispersant.

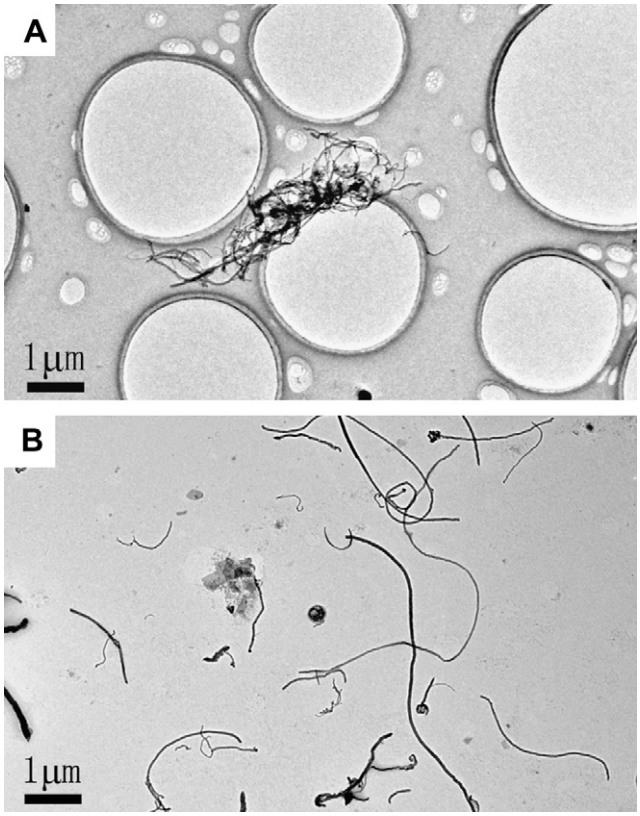


**Fig. 5.** TEM images of dried MWNT dispersions after high-shear homogenizing, ultrasonication in toluene: A) without any dispersant; B) with 9BA-4-9BA as dispersant.

### 3.3. Presence of gemini surfactant in PS/MWNT nanocomposite

Considering the solubility of the 9BA-4-9BA in ethanol at 25 °C, 4.22 g/100 g, is much larger than that in toluene, 0.12 g/100 g, the 9BA-4-9BA molecules might be removed from the PS/MWNT nanocomposites during the precipitation process using ethanol (section 2.4). In order to check whether the gemini surfactant still remained in the as-prepared PS/MWNT nanocomposites, a Soxhlet extraction and subsequent FTIR spectra measurement were performed. The extracted solution was concentrated and then dried on KBr pellet for FTIR studies. The FTIR spectra are shown in Fig. 7, and the tentative band assignments are illustrated in Table 2. The

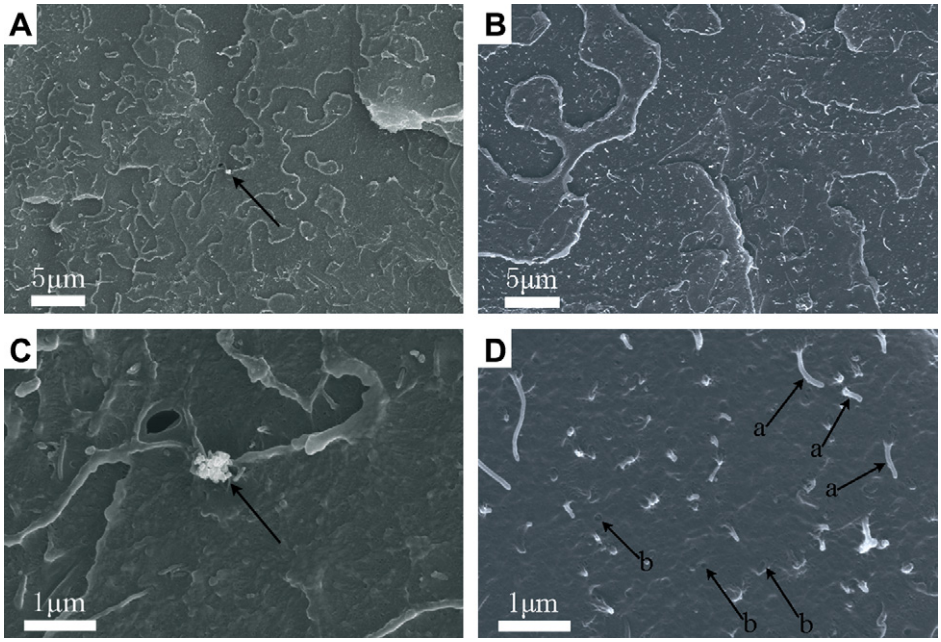


**Fig. 6.** Representative SEM images of PS/MWNT composite (A and C, without any dispersant) or nanocomposite (B and D, with the 9BA-4-9BA as dispersant) containing of 1 wt% MWNTs.

broad band around 3440 $cm^{-1}$ may be assigned to the –OH stretching of $–SO_3H$ groups in the 9BA-4-9BA. The absorption bands at 2920 and 2852 $cm^{-1}$ are ascribed to the $–CH_2$ asymmetric and symmetric stretching, respectively. The bands at 1463 and 1020 $cm^{-1}$ result from the benzene ring, while 1260 $cm^{-1}$ is attributed to the S–O stretching of the gemini surfactant $–SO_3H$ anions. It is obvious that the –OH group and S–O stretching modes of the gemini surfactant occur in Fig. 7B. This confirms the presence of the gemini surfactant in the as-prepared PS/MWNT nanocomposite. Moreover, according to the mass decrease of the PS/MWNT nanocomposite after the extraction, we can measure that the weight percent of the remained gemini surfactant in the nanocomposite is 4.28 wt%.

### 3.4. Nanocomposite properties

#### 3.4.1. Conductivity

In light of the greatly improved dispersion of MWNTs, the PS/MWNT nanocomposite is expected to have much more conductive networks, and thus exhibits greatly enhanced electrical conductivity even at low MWNT loading. To this end, conductivity measurements were carried out using the film samples with an average thickness of 10 μm by evaporating toluene of the nanocomposite dispersion on glass slides. Table 3 reveals that with the addition of a small amount of MWNTs, the electrical conductivity increases very sharply from around $10^{-16–20}$ S $m^{-1}$ of neat PS to larger than $10^{-3}$ S $m^{-1}$ of the composite or nanocomposite, due to the excellent conductivity of MWNTs. More importantly, the PS/MWNT nanocomposite containing 9BA-4-9BA as dispersant has much higher conductivity than that of the corresponding PS/MWNT composite at the same MWNT content. At MWNT loading of only 1.0 wt%, the PS/MWNT nanocomposite in the presence of 9BA-4-9BA has a drastic increase of conductivity of even larger than 800 times of the corresponding PS/MWNT composite. The significantly debundling and homogeneous dispersion of the MWNTs improved by the 9BA-4-9BA surfactant may be one major factor to such dramatically increase of conductivity. In addition, the presence of the $–SO_3H$ groups of the gemini surfactant may also contribute to the enhanced conductivity. According to the Soxhlet extraction, the content of 9BA-4-9BA remained in the PS/MWNT nanocomposite is 4.28 wt%. For comparison, a PS/9BA-4-9BA mixture containing of the same 9BA-409BA amount was determined to have a conductivity of 0.0061 S $m^{-1}$. This reveals the contribution of the 9BA-4-9BA to the nanocomposite conductivity. Indeed, the present publications present a striking variation in measured values of the polymer/CNT nanocomposite electrical conductivity [39–43]. The disparity depends on many factors, such as the structure and quality of the used MWNTs, the contents of amorphous carbon and catalyst particles, the difference of the surface organic modification, etc. Here, we aim at the effect of the gemini surfactant on MWNT dispersion in PS and the

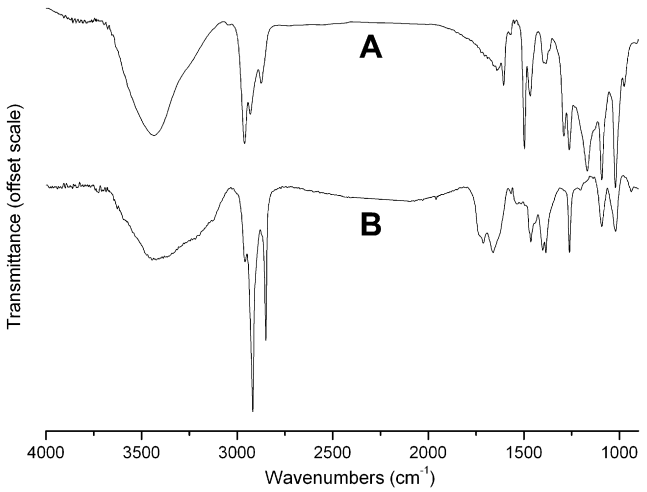


**Fig. 7.** FTIR spectra of A) 9BA-4-9BA; B) dried sample of the PS/MWNT nanocomposite Soxhlet extracted solution.

**Table 2**
FTIR band assignments of the dried sample of PS/MWNT nanocomposite Soxhlet extracted solution.

| Wavenumber/cm$^{-1}$ | Tentative assignment |
|---|---|
| 3440 | –OH stretching |
| 2920 | –$CH_2$ asymmetric stretching |
| 2852 | –$CH_2$ symmetric stretching |
| 1463 | $\delta(CH_2)$, $\nu_{19}$(B1) |
| 1260 | S–O stretching of $SO_3H$ |
| 1020 | $\nu_{18A}$(A1) |

corresponding electrical conductivity. We conclude that the gemini surfactant can greatly improve the dispersion of MWNT in PS and the conductivity.

### 3.4.2. Thermal stability

Thermal stability is very important for polymeric materials. In polymer/inorganic composites or hybrids, organic molecules are often adopted as surface modifying agents to lower the surface energy, improve the dispersion of the inorganic particles and also benefit the compatibility of polymer matrix with inorganic component. Nevertheless, the introduction of the organic surface modifiers often results in an inferior polymer thermal stability due to their low thermal stability. For example, the amine cations have been reported to induce and accelerate the thermal [44] and photo [45] degradation of PP in PP/clay nanocomposites. In the present study, TGA was performed to evaluate the thermal stability. The results are shown in Fig. 8. When the heating rate is 20 °C/min (as shown in Fig. 8A), the 9BA-4-9BA degrades at 181.2 °C in nitrogen atmosphere, and the small weight loss at 84.6 °C results from evaporation of adsorbed water. Fortunately, the application of the 9BA-4-9BA does not have a detrimental effect on the thermal stability of PS. Indeed, the PS/MWNT nanocomposite exhibits an enhanced thermal property compared with neat PS. The onset decomposition temperature increases from 408.7 °C of the neat PS to 417.2 °C of the surfactant-containing nanocomposite. When the heating rate is 10 °C/min (shown in Fig. 8B), the PS/MWNT nanocomposite also shows an increased thermal stability relative to that of the neat PS. Its onset decomposition temperature is 404.6 °C, obviously higher than that of the neat PS, 390.5 °C.

### 3.4.3. Tensile properties

The tensile properties of the PS/MWNT nanocomposite films are illustrated in Table 4 and Fig. 9. When bare MWNTs were added, the PS/MWT composites possess decreased mechanical properties including tensile strength, elongation at break and tensile modulus, except the elongation at break at 0.25 wt%. As for the nanocomposite, it has an obvious increase of tensile modulus at low MWNT content of 0.25 wt%, about 12% higher than that of the neat PS at this MWNT content. Other mechanical properties are comparable to or less than that of the neat PS. The effect of MWNTs on the mechanical of the PS/MWNT composites or nanocomposites

**Table 3**
Conductivities of PS//MWNT nanocomposite (1.0 wt%), PS/MWNT composite (1.0 wt%), PS and PS/9BA-4-9BA (4.28 wt%).

| | Conductivity |
|---|---|
| PS/MWNT nanocomposite[a] [S m$^{-1}$] | 4.3 |
| PS/MWNT composite[b] [S m$^{-1}$] | 0.0053 |
| PS[c] | $10^{-16-20}$ |
| PS/9BA-4-9BA | 0.0061 |

[a] Containing of 9BA-4-9BA as dispersing agent.
[b] Without 9BA-4-9BA.
[c] Cited from literatures [37,38].

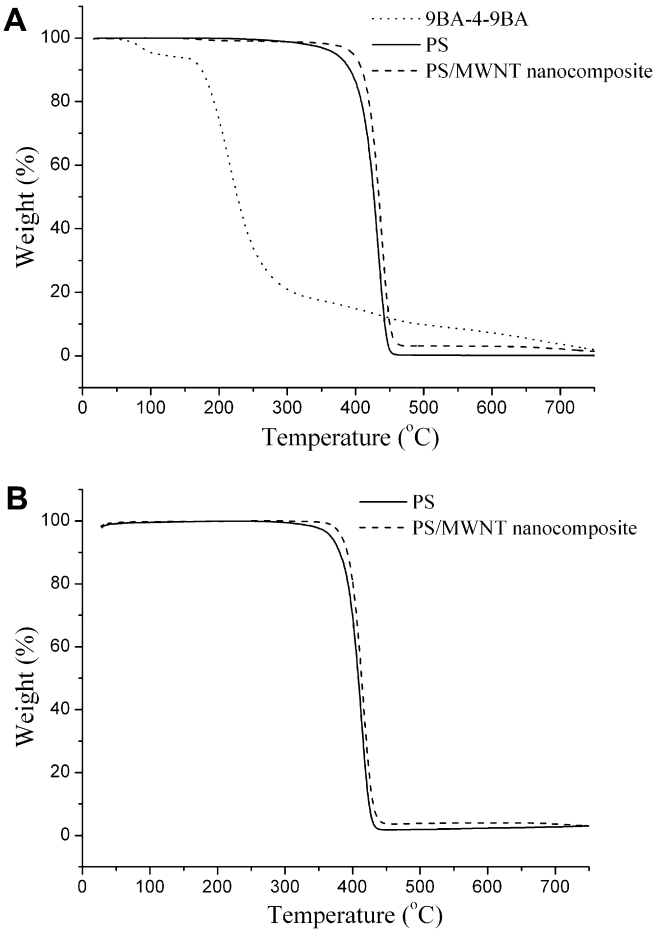


**Fig. 8.** TGA curves of PS, 9BA-4-9BA and PS/MWNT nanocomposite (containing of 1 wt% MWNT), heating rate: A, 20 °C/min; B, 10 °C/min.

may be complex. The residue of the gemini surfactant, MWNT dispersion state, MWNT structure and perfection, and the interfacial interaction between PS and MWNTs may play important roles. The bare MWNTs resulted in decrease of the mechanical properties, wherein the poor dispersion and large bundles of MWNTs (as shown in Fig. 5A and C) may be the main reason. In the nanocomposites, although the nanoscale dispersion of MWNTs will definitely increase the mechanical properties, the residue of the gemini surfactant, a plasticizer of PS, has detrimental effect on the mechanical properties. Additionally, besides many MWNTs ebbeded in the PS matrix, a few holes pointed by arrows b are

**Table 4**
The tensile properties of PS/MWNT nanocomposites or composites at different MWNT content.

| | MWNT content/wt% | Tensile strength/MPa | Elongation at break/% | Modulus/MPa |
|---|---|---|---|---|
| PS | 0 | 30.6 ± 2.8 | 2.5 ± 0.2 | 2125 ± 167 |
| PS/MWNT nanocomposite[a] | 0.25 | 30.3 ± 1.5 | 2.4 ± 0.1 | 2371 ± 59 |
| | 0.50 | 25.3 ± 0.3 | 2.6 ± 0.4 | 1862 ± 19 |
| | 1.0 | 25.1 ± 1.3 | 2.3 ± 0.6 | 1943 ± 75 |
| PS/MWNT composite[b] | 0.25 | 25.2 ± 1.8 | 2.7 ± 0.2 | 1898 ± 155 |
| | 0.50 | 24.3 ± 0.7 | 2.4 ± 0.1 | 2026 ± 178 |
| | 1.0 | 25.8 ± 2.1 | 2.0 ± 0.5 | 1944 ± 73 |

[a] Containing of 9BA-4-9BA as dispersing agent.
[b] Without 9BA-4-9BA.

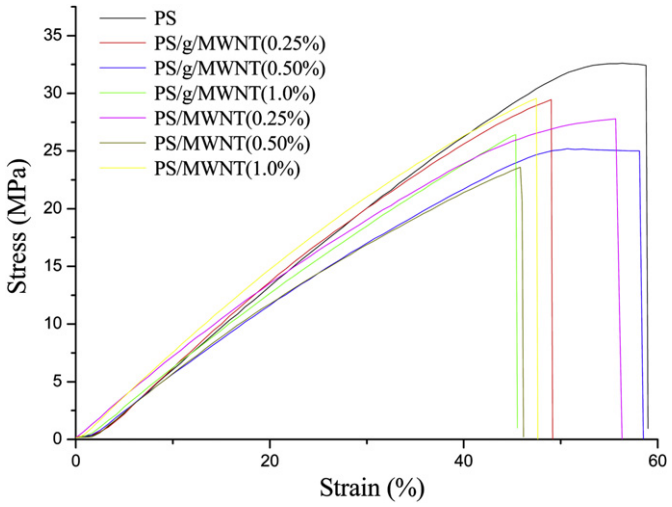


**Fig. 9.** Tensile testing curves of the PS/MWNT nanocomposites and composites with different MWNT content, wherein the abbreviations of PS/g/MWNT and PS/MWNT represent PS/MWNT nanocomposite and composite, respectively.

present in Fig. 6D, indicating that the interfacial interaction between MWNTs and PS, i.e., the noncovalent wrapping, is not very strong. As a result, the overall mechanical properties of the PS/MWNT nanocomposite do not exhibit an obvious increase except the tensile modulus at 0.25 wt%.

## 4. Conclusion

In summary, we have developed a new facile and effective route to disperse MWNTs in organic solvent and further prepare PS/MWNT nanocomposite using a gemini surfactant. The nanocomposite exhibits enhanced electrical conductivity and thermal stability. Although only PS and MWNTs were employed in the present study, this work may open new avenues to dispersion of CNTs including single-walled CNTs (SWNTs) in diverse organic solvents and expand to preparation of other polymer/CNT nanocomposites aided by optimal molecular design of gemini surfactants.

## Acknowledgments

The authors thank financial support by the National Natural Science Foundation of China (No. 50873103). G. Chen acknowledges the support of K. C. Wong Education Foundation, Hong Kong and Beijing Nova Program (No. 2007A087).

## References

[1] Ijima S. Nature 1991;354:56–8.
[2] Yu MF, Lourie O, Dyer MJ, Monoli KM, Kelly TF, Ruoff RS. Science 2000;287:637–40.
[3] Grimes CA, Dickey EC, Mungle C, Ong KG, Qian D. J Appl Phys 2001;9:4134–7.
[4] Berber S, Kwon YK, Tomank D. Phys Rev Lett 2000;84:4613–6.
[5] Thess A, Lee R, Nikolaev P, Dai H, Petit P, Robert J, et al. Science 1996;273:483–7.
[6] Hu H, Zhao B, Itkis ME, Haddon RC. J Phys Chem B 2003;107:13838–42.
[7] Shaffer M, Fan X. Carbon 1998;36:1603–12.
[8] Velasco-Santos C, Martínez-Hernádez AL, Fisher FT, Ruoff R, Castaño VM. Chem Mater 2003;15:4470–5.
[9] Haggenmueller R, Gommans H. Chem Phys Lett 2000;330:219–25.
[10] Chen J, Hamon MA, Hu H, Chen Y, Rao AM, Eklund PC, et al. Science 1998;282:95–8.
[11] Qin Y, Liu L, Shi J, Wu W, Zhang J, Guo Z, et al. Chem Mater 2003;15:3256–60.
[12] Putz K, Krishnamoorti R, Green PF. Polymer 2007;48:3540–5.
[13] Chen G-X, Kim H-S, Park BH, Yoon J- S. Polymer 2006;47:4760–7.
[14] Jeon J-H, Lim J-H, Kim K-M. Polymer 2009;50:4488–95.
[15] Vaisman L, Wagner H. Adv Colloid Interface Sci 2006;128–130:37–46.
[16] Islam MF, Rojas E, Bergey DM, Johnso AT, Yodh AG. Nano Lett 2003;3:269–73.
[17] Vaisman L, Maron G, Wagner HD. Adv Funct Mater 2006;16:357–63.
[18] Haggenmueller R, Du F, Fischer JE, Winey KI. Polymer 2006;46:2381–8.
[19] O'Connel MJ, Bachilo SM, Huffman CB, Moore VC, Strano MS, Haroz EH, et al. Science 2002;297:593–6.
[20] Sun Z, Nicolosi V, Rickard D, Bergin SD, Aherne D, Coleman JN. J Phys Chem C 2008;112:10692–9.
[21] Liu J, Rinzler AG, Dai H, Hafner JH, Bradley RK, Boul PJ, et al. Science 1998;280:1253–6.
[22] Zhang X, Liu T, Sreekumar TV, Kumar S, Moore VC, Hauge RH, et al. Nano Lett 2003;3:1285–8.
[23] Star A, Stoddart JF, Steuerman D, Diehl M, Boukai A, Wang EW, et al. Angew Chem Int Ed 2001;40:1721–5.
[24] Star A, Steuerman DW, Heath JR, Stoddart JF. Angew Chem Int Ed 2002;41:2508–12.
[25] Yuan J-M, Fan Z-F, Chen X-H, Chen X-H, Wu Z-J, He L-P. Polymer 2009;50:3285–91.
[26] Dyke CA, Tour JM. Chem Eur J 2004;10:812–7.
[27] Anderson RE, Barron AR. J Nanosci Nanotechn 2007;7:3426–40.
[28] Bellayer S, Gilman J, Eidelman N, Bourbigot S, Flambard X, Fox DM, et al. Adv Funct Mater 2005;15:910–6.
[29] Menger FM, Littau CA. J Am Chem Soc 1991;113:1451–2.
[30] Menger FM, Keiper JS. Angew Chem Int Ed 2000;39:1906.
[31] Zana R. J Colloid Interface Sci 2002;248:203–20.
[32] Menger FM, Littau CA. J Am Chem Soc 1993;115:10083–90.
[33] Shi L, Lundberg D, Musaev DG, Menger FM. Angew Chem Int Ed 2007;46:5889–91.
[34] Xie J, Yang J, Chen G, Chen X. Langumir 2009;25:6100–5.
[35] Wang Q, Han Y, Wang Y, Qing Y, Guo Z. J Phys Chem B 2008;112:7227–33.
[36] Chen L, Xie H, Yang L, Yu W. Colloids Surf A 2008;330:176–9.
[37] Chang TE, Kisliuk A, Rhodes SM, Brittain WJ, Sokolov AP. Polymer 2006;47:7740–6.
[38] Kota A, Cipriano BH, Duesterberg MK, Gershon AL, Powell D, Raghavan SR, et al. Macromolecules 2007;40:7400–6.
[39] Grossiord N, Loos J, Regev O, Koning CE. Chem Mater 2006;18:1089–99.
[40] Grunlan JC, Mehrabi AR, Bannon MV, Bahr JL. Adv Mater 2004;16:150–3.
[41] Grossiord N, Loos J, van Laake L, Maugey M, Zakri C, Koning CE, et al. Adv Funct Mater 2008;18:3226–34.
[42] Mazinani S, Ajji A, Dubois C. Polymer 2009;50:3329–42.
[43] Mu M, Walker AM, Torkelson JM, Winey KI. Polymer 2008;49:1332–7.
[44] Zanetti M, Camino G, Reichert P, Mülhaupt R. Macromol Rapid Commun 2001;22:176–80.
[45] Qin H, Zhao C, Zhang S, Chen G, Yang M. Polym Degrad Stab 2003;81:497–500.